Chemical Geology xxx (2016) xxx–xxx

Contents lists available at ScienceDirect

Chemical Geology

journal homepage: www.elsevier.com/locate/chemgeo

Thermodynamic modeling of Mn(II) adsorption onto manganese oxidizing bacteria

Angélica Vázquez-Ortega *, Jeremy B. Fein

Department of Civil & Environmental Engineering & Earth Science, University of Notre Dame, Notre Dame, IN 46556, USA

ARTICLE INFO

Article history:
Received 14 October 2016
Received in revised form 23 December 2016
Accepted 28 December 2016
Available online xxxx

Keywords:
Surface complexation modeling
Bacteria
Metal adsorption
Manganese

ABSTRACT

Bacterial cell membranes display a strong affinity for a wide variety of aqueous metal cations and have the potential to affect the mass transport of these cations through adsorption reactions in water–rock systems. Prior studies have focused on determining the thermodynamic stability constants of heavy metals and radionuclides; however, the constants for Mn-bacterial surface complexes formed on manganese oxidizing bacteria remain unmeasured. We measured the rate, extent, and reversibility of Mn(II) adsorption onto a bacterial species capable of Mn-oxidization (*Pseudomonas putida*), and onto a bacterial species that does not promote Mn-oxidization (*Bacillus subtilis*). The extent of adsorption was measured as a function of both pH and metal loading in order to determine the thermodynamic stability constants of the Mn-bacterial surface complexes that form on the bacteria and to test whether Mn oxidizers exhibit unusual Mn adsorption behavior relative to species that do not oxidize Mn. Furthermore, we determined the effect of bacterial extracellular polymeric substances (EPS) on Mn(II) adsorption by conducting experiments with and without EPS removal from the biomass. The experimental results indicated that Mn(II) adsorption onto *B. subtilis* and *P. putida* was rapid and reversible. The extent of Mn(II) adsorption onto both bacterial species increased with increasing pH, but *P. putida* adsorbed significantly more Mn(II) than did *B. subtilis* across most of the pH range studied. Both the adsorption measurements and the calculated stability constants indicate that *P. putida*, a Mn oxidizing bacterial species, exhibited significantly enhanced Mn adsorption relative to that observed for *B. subtilis*. The enhanced Mn(II) adsorption exhibited by *P. putida* suggests that bacteria may adapt the metal binding environments within their cell envelopes in order to optimize bioavailability of metals that are beneficial to their metabolism. Experiments conducted at low metal-loading conditions yielded stability constants for the Mn(II)-bacterial surface complexes that were less than or similar to those calculated for the high metal-loading conditions, suggesting that Mn(II)-sulfhydryl binding does not dominate under low metal loading conditions as it does for other metals. Removal of EPS molecules from *P. putida* led to significantly reduced extents of Mn(II) adsorption, suggesting that Mn(II)-EPS binding plays at least some role in the overall adsorption of Mn(II) onto *P. putida* biomass.

1. Introduction

Bacteria play an integral role in the biogeochemical cycling of a wide range of metals in low temperature bacteria-bearing systems. Because adsorption is the first step in metal bioavailability for many processes (Fein, 2016), it is crucial to determine the identities and thermodynamic stabilities of metal-bacteria surface complexes in order to construct rate laws for metabolic processes that involve metals. Bacterial cell envelopes display a strong affinity to adsorb a wide variety of aqueous metal cations due to the presence of metal-binding functional groups such as carboxyl, phosphoryl, amino, and sulfhydryl sites (e.g., Kelly et al., 2001; Boyanov et al., 2003; Yu and Fein, 2015). Cell envelope metal adsorption not only can affect the transport and fate of aqueous metals in geologic systems (Czajka et al., 1997; Yee and Fein, 2002; Wu et al., 2006), but also can control metal bioavailability in general (Borrok and Fein, 2005; Sheng et al., 2011; Flynn et al., 2014).

Previous studies of metal adsorption onto bacteria have involved mostly heavy metals and radionuclides in order to determine the effect of bacterial adsorption on the environmental fate of these elements (e.g., Plette et al., 1996; Fein et al., 1997; Ngwenya et al., 2003; Guiné et al., 2006; Gonzalez et al., 2014; Huang et al., 2014). For example, Plette et al. (1996) studied the adsorption of Cd onto isolated cell membranes of a Gram-positive soil bacterium. The binding mechanism in the absence of Ca and at low Cd concentrations was mainly controlled by the formation of Cd-carboxyl complexes. Site specific stability constants for metal-bacteria surface complexes (e.g., Cd, Cu, Pb, and Al) have been determined by using surface complexation modeling (Fein et al., 1997). Ngwenya et al. (2003) reported that carboxyl and phosphoryl sites on

* Corresponding author.
E-mail address: avazque3@nd.edu (A. Vázquez-Ortega).

http://dx.doi.org/10.1016/j.chemgeo.2016.12.040
0009-2541/

the cell membranes of a Gram-negative bacterium were involved in Zn and Pb uptake. The Fe-binding sites onto the cell membrane of *Pseudomonas aureofaciens* were investigated by using Fe K-edge X-ray absorption fine structure spectroscopy (Gonzalez et al., 2014) and the results suggested that Fe adsorption was dominated by phosphoryl moieties with carboxyl sites also playing a role.

To our knowledge, all previous studies of metal adsorption onto bacteria have involved metals that are not used by the bacteria for beneficial purposes. In this study, we test whether *P. putida* has an especially high affinity to adsorb Mn relative to other bacteria due to the potential physiological benefits of Mn(II) to the organism (Tebo et al., 2005, 2010; Geszvain et al., 2012). Mn(II) oxidation by the wild type *Pseudomonas putida* GB-1 has been linked with maintaining physiological processes in the cell, and with the cell's ability to reduce oxidative stress (Banh et al., 2013). Furthermore, bacterial Mn(II) oxidation leads to the formation of Mn(IV) oxides which can act as electron acceptors, oxidize organic carbon compounds, serve as protective shields against external reactive oxygen species, and through adsorption can reduce the toxicity of a range of heavy metals and radionuclides to the cell (Tebo et al., 2005, 2010; Geszvain et al., 2012; Banh et al., 2013). In this study, we measured Mn(II) adsorption onto a bacterial species capable of Mn-oxidation (*P. putida*) and onto a bacterial species (*B. subtilis*) that exhibits metal adsorption behavior representative of a wide range of other bacteria (Yee and Fein, 2001) in order to test whether a Mn-oxidizer exhibits anomalous Mn(II) adsorption behavior. We measured the adsorption behavior as a function of both pH and metal loading at a fixed ionic strength, and we used the results to constrain the thermodynamic stability constants for the important Mn-bacterial surface complexes. The results indicate that *P. putida* exhibits enhanced Mn(II) adsorption, and we conducted a series of experiments that were designed to test whether sulfhydryl or bacterial extracellular polymeric substances (EPS) binding play a role in this unique adsorption behavior. *P. putida* produces large amounts of EPS, which is primarily composed of glycerol, acetylated amino sugars, and xylose (Celik et al., 2008). Several studies have postulated the importance of EPS to the environmental distribution and bioavailability of metals in bacteria-bearing geologic systems (e.g., Czajka et al., 1997; Jensen-Spaulding et al., 2004; Yang et al., 2013), and numerous studies have characterized the metal binding capacity of bacterial EPS, demonstrating that significant concentrations of binding sites are present on EPS molecules (Liu and Fang, 2002; Guibaud et al., 2005; Huang et al., 2011; Kantar et al., 2011; Wei et al., 2011; Gutierrez et al., 2012). However, contrasting results on the effects of EPS on metal adsorption onto bacterial biomass have been reported (Tourney et al., 2009; Baker et al., 2010; Gonzalez et al., 2010; Fang et al., 2011; Kenney and Fein, 2011). Some studies report enhanced metal adsorption in the presence of EPS (Raungsomboon et al., 2006; Baker et al., 2010; Fang et al., 2011; Wei et al., 2011), while some report negligible (Ueshima et al., 2008; Tourney et al., 2009; Kenney and Fein, 2011) or even negative effects (Gonzalez et al., 2010) of the EPS on the extent of metal adsorption onto bacteria. The objectives of this study are to determine whether a Mn(II)-oxidizing bacterial species exhibits enhanced Mn(II) adsorption behavior relative to a non-Mn(II)-oxidizing species, and whether EPS produced by *P. putida* exerts a significant effect on the Mn(II) adsorption behavior.

2. Materials and methods

2.1. Bacteria cell preparation

Pseudomonas putida (ATCC# 33015) and *Bacillus subtilis* (ATCC# 6051) cells were cultured aerobically. All growth media and experimental solutions that were used in this study were made with ultrapure 18 MΩ water. The bacterial cells were first transferred from an agar plate to a test tube containing 3 mL of autoclaved trypticase soy broth (TSB) with 0.5% yeast extract, and incubated at 32 °C for 24 h. The cell suspension in the tube was then transferred to 2 L of autoclaved TSB with 0.5% yeast extract, and incubated at 32 °C for another 24 h until a stationary growth phase was attained. Cells were collected by centrifugation at 8100*g* for 5 min. Collected cells were then rinsed three times in 0.1 M $NaClO_4$ and the pellets were recollected by centrifugation at 8100*g* for 5 min after each rinse. After the three rinses, and the cells were then centrifuged twice at 8100*g* for 0.5 h without any further addition of 0.1 M $NaClO_4$, with the supernatant being discarded after each 0.5 h period, and the mass of the resulting cell pellet (termed 'wet weight' hereafter) was measured. The wet weight to dry weight conversion ratios for these bacterial species were measured by drying approximately 2 g (wet weight) of washed biomass at 100 °C for 24 h until the weight did not change with time. The resulting ratios of wet weight to dry weight are 4.5 for *P. putida* and 4.7 for *B. subtilis*.

2.2. Adsorption experiments

Mn(II) adsorption experiments were conducted using washed *P. putida* and *B. subtilis* cells under anoxic conditions to ensure little or no oxidation of the aqueous Mn(II), following a procedure similar to that described by Yu and Fein (2016). All experiments in this study were conducted inside a glovebox chamber with a gas composition of 95% N_2/5% H_2. Experimental solutions containing 0.1 M $NaClO_4$ and 4 mg L^{-1} Mn(II) (introduced as a $Mn(ClO_4)_2$ salt) were first bubbled with 95% N_2/5% H_2 for 0.5 h. The pH was initially adjusted to 6.5 using small aliquots of concentrated HNO_3 or NaOH. Solutions and harvested washed cells were transferred into the glovebox. Before the addition of bacterial cells to the experimental solutions, samples were taken in order to determine the initial total dissolved manganese concentration. A known weight of cells was added to weighed volumes of 0.1 M $NaClO_4$ electrolyte solutions containing 4 mg L^{-1} of Mn(II) to form a parent cell suspensions with a metal:biomass ratio of 3.6 μmol Mn/g wet cells. We conducted adsorption equilibrium experiments as a function of time, pH, and Mn loading and we also conducted desorption equilibrium experiments. In each approach, approximately 10 mL aliquots of a parent bacteria-Mn(II)-electrolyte suspension were transferred to a series of 50 mL centrifuge tubes containing small aliquots of HNO_3 or NaOH to control pH, and the tubes were placed on a rotating rack with no further pH adjustment. After the equilibration period, pH was measured prior to sampling the solution. In all sampling approaches, the experimental suspensions were centrifuged at 8100*g* for 5 min and filtered through a 0.45 μm nylon membrane. Filtered solutions were acidified using one drop of 16 N nitric acid and the concentration of total Mn remaining in solution was determined by inductively coupled plasma optical emission spectroscopy (ICP-OES) at a wavelength of 257.610 mm, with matrix-matched calibration standards. Machine drift was checked by analyzing standards before, during and after analysis of the experimental samples. Analytical uncertainty, determined by repeat analyses of the standards, was $<\pm 2\%$. The extent of adsorption was taken to be the difference between the starting and final aqueous Mn concentrations.

Experimental controls were conducted to determine the potential for abiotic Mn(II) oxidation under the experimental conditions. Biomass-free control experiments were conducted using solutions containing 0.1 M $NaClO_4$ and 4 mg L^{-1} of Mn(II) at various pH values (4.5, 5.5, 6.5 and 7.5), and samples were taken as a function of time over 4 h. Results revealed negligible loss of Mn(II) from the system (Fig. S1, Supplemental Material). For the adsorption kinetics experiments, samples were collected after 0.5, 1, 2, 3, and 4 h of reaction time. The adsorption kinetics exhibited by *B. subtilis* and *P. putida* differ in a number of ways (Fig. S2, Supplemental Material). *P. putida* exhibited a much faster attainment of steady-state than did *B. subtilis*. The *P. putida* experiments were at steady-state by the time the first sample was taken at 0.5 h, whereas the *B. subtilis* system took approximately 3–4 h to reach steady-state under the experimental conditions. Secondly, *P. putida* exhibited a slight but significant enhancement of the extent of Mn(II) adsorption relative to *B.*

Please cite this article as: Vázquez-Ortega, A., Fein, J.B., Thermodynamic modeling of Mn(II) adsorption onto manganese oxidizing bacteria, Chem. Geol. (2016), http://dx.doi.org/10.1016/j.chemgeo.2016.12.040

subtilis. Based on the results of the kinetics experiments, all subsequent Mn(II) adsorption experiments involving *B. subtilis* and *P. putida* were equilibrated for 4 and 2 h, respectively.

The reversibility of Mn(II) adsorption onto both species was tested with desorption experiments in which bacteria-Mn(II)-electrolyte suspensions first were reacted for 4 h for *B. subtilis* and 2 h for *P. putida* at pH 7.5. This pH was chosen to maximize Mn adsorption onto both bacterial species so that after the initial equilibration period at high pH, the pH of the experimental solutions could be adjusted downward, forcing desorption of Mn from the bacterial cells and thereby testing the reversibility of the adsorption reaction. After the initial adsorption step, the suspensions were transferred into separate test tubes, and the pH was adjusted downward to promote desorption using small aliquots of nitric acid to a range of pH 3 to 7. Samples were then taken as described above and analyzed for dissolved total Mn using ICP-OES. Full reversibility was attained after 2 h for *P. putida*, and after 6 h for *B. subtilis*, with the exception of the low pH systems for the *P. putida* experiments (below pH 4).

Further control experiments including biomass were conducted to test whether *P. putida* or *B. subtilis* have the ability to oxidize Mn(II) under the anoxic experimental conditions (Fig. S3, Supplemental Material). These control experiments were performed in a similar fashion to the desorption experiments; Mn(II) was adsorbed onto the biomass at pH 7.5 and allowed to equilibrate for 2 h. Samples were taken and then each system was acidified to pH 2 with addition of nitric acid, and allowed to re-equilibrate for 2 h, promoting Mn desorption from the biomass. All samples were centrifuged, and total aqueous Mn concentrations were measured by ICP-OES, and aqueous Mn(II) concentrations were measured using a formaldoxime colorimetric procedure (Armstrong et al., 1979). The Mn(II) concentrations were determined by a UV–Vis spectrophotometer (Cary 300 Bio) at a wavelength of 300 nm. The initial (prior to adsorption) and final (after acidification) concentrations of total Mn and Mn(II) in solution were all identical within analytical uncertainties (Fig. S3). The percentage of total Mn and Mn(II) adsorbed onto the *B. subtilis* and *P. putida* cells during the adsorption step was 70% and 90%, respectively. These results indicate that Mn remains as Mn(II) in solution under the experimental conditions, and that adsorption onto the bacteria does not lead to Mn(II) oxidation to a significant degree, as the Mn that desorbed from the bacteria was entirely Mn(II).

Additional experiments with metal:biomass ratios ranging from approximately 0.5 to 40 μmol Mn/g (wet mass) bacteria were conducted using only *P. putida* (Table S1, Supplemental Material). In these experiments, the bacterial wet weight and Mn(II) concentrations were varied to obtained the desired metal:biomass ratios (Table S1, Supplemental Material). The final pH measurement, sample centrifugation and filtration and total Mn analysis by ICP-OES were performed as previously described. In addition to measuring the adsorption behavior as a function of pH and metal:biomass ratios, we also measured the effect of bacterial extracellular polymeric substances (EPS) on the extent of Mn(II) adsorption onto *P. putida*. *P. putida* produces extensive EPS and hence is an ideal species for studying the effects of EPS on metal adsorption behavior. We conducted similar Mn(II) adsorption experiments to those described above, except EPS molecules were removed and washed away from the bacterial cells using procedures described previously (Sheng et al., 2005; Yu and Fein, 2016). Briefly, the removal of EPS from the freshly harvested and rinsed cell pellets was accomplished by re-suspension of the biomass pellet in 0.1 M $NaClO_4$ with 2% (mass/mass) EDTA (disodium salt, 0.6 g of EDTA/g of biomass). The solution was allowed to react for 2 h at room temperature (~20 °C) with slow stirring in order to maintain homogeneous suspensions. EDTA cleaves EPS molecules from the bacterial cells, and the EDTA and EPS molecules were then rinsed away following the same rinsing protocol described above. Adsorption experiments were conducted with the EPS-free cells as described above with pH ranging from 4 to 8, and metal:biomass ratios ranging from approximately 0.5 to 40 μmol Mn/g (wet weight) bacteria.

3. Results and discussion

3.1. Mn(II) adsorption experiments

The results from the Mn(II) adsorption experiments conducted as a function of pH for *B. subtilis* and *P. putida* with a metal:biomass ratio of 3.6 μmol Mn/g wet cells are presented in Fig. 1. In both bacterial systems, the adsorption exhibited a strong pH dependence, with the extent of adsorption generally increasing with increasing pH. The extent of adsorption plateaus in the *P. putida* system at approximately pH 6.2 at 87%. The *B. subtilis* system exhibited a shallower pH dependence to the adsorption above pH 5.5, but did not attain a plateau. The extent of Mn(II) adsorption onto *P. putida* was enhanced relative to that observed onto *B. subtilis* across most of the pH range of interest, with the greatest enhancement in the mid-pH range studied (pH 5 to 7) (Fig. 1). For instance, *P. putida* adsorbed approximately 9% more Mn than did *B. subtilis* at pH 3.5, approximately 32% more at pH 5.5, and approximately 9% more at pH 7.0. The adsorption enhancement by *P. putida* cannot be attributed to changes in Mn oxidation state at the high pH values included in this study, since both the biotic and abiotic control experiments indicated that Mn remained as Mn(II) for the duration of the experiments. Although the pH 3.8 data point appears anomalous, in general the lower pH data (below pH 4) suggest that desorption was incomplete. A possible explanation for the lack of reversibility in the low pH *P. putida* systems is that protonation of functional groups within the EPS molecules and other cellular exudates under low pH conditions could lead to hydrophobic-driven aggregation and trapping of bound Mn within the aggregates, making its release more difficult and slow than under higher pH conditions.

The effects of the experimental Mn:biomass ratio and of EPS removal on the extent of Mn(II) adsorption onto *P. putida* as a function of pH are depicted in Fig. 2. The highest extents of Mn(II) adsorption were observed under the lowest metal loading conditions, with a greater dependence on the Mn:biomass ratio observed in the experiments that involved intact EPS molecules. In addition, the removal of EPS caused a significant decrease in the extent of Mn(II) adsorption, with the effect largest between pH values of approximately 5.0 and 6.5. For example, in the experiments with intact EPS, at metal loading conditions of 0.5 and 40 μmol Mn/g wet cells and at pH 6.0, the observed extent of Mn(II) adsorption was 88% and 45%, respectively. In the experiments involving EPS-free cells, under the same metal loading and pH conditions, the observed Mn(II) adsorption values were 39% and 12%, respectively. Our results indicate that EPS binding plays a substantial role in the observed Mn(II) adsorption behavior.

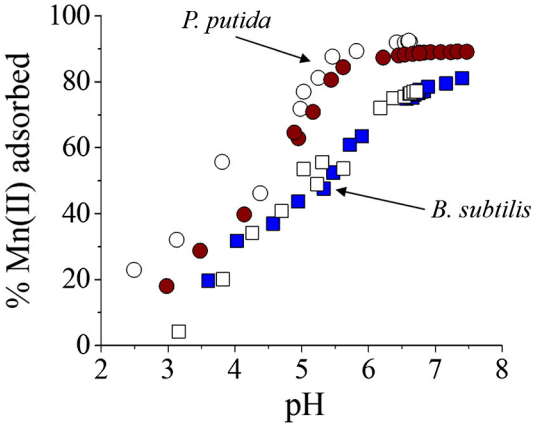

Fig. 1. Measured extent of Mn(II) adsorption (filled symbols) and desorption (open symbols) as a function of pH for *B. subtilis* (squares) and *P. putida* (circles). This experiments were conducted with a metal:biomass ratio of 3.6 μmol Mn/g wet cells.

Please cite this article as: Vázquez-Ortega, A., Fein, J.B., Thermodynamic modeling of Mn(II) adsorption onto manganese oxidizing bacteria, Chem. Geol. (2016), http://dx.doi.org/10.1016/j.chemgeo.2016.12.040

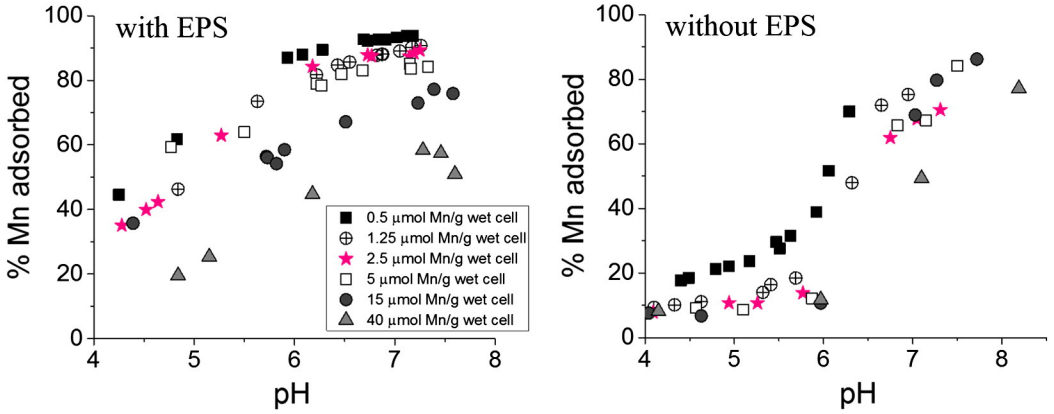

Fig. 2. Mn(II) adsorption onto *P. putida* as a function of both pH and metal loading conditions. The left panel depicts the data for *P. putida* with EPS molecules intact, and the right panel shows the data for *P. putida* with the EPS removed.

3.2. Surface complexation modeling

Surface complexation modeling was used to determine the Mn(II)-bacterial complexes that form under the experimental conditions and to constrain their thermodynamic stability constants. The bacterial surface protonation and Mn(II) complexation reactions were modeled using a non-electrostatic four proton-active site model (Yu et al., 2014). Borrok and Fein (2005) demonstrated that bacterial surface electric field effects are negligible for proton and metal adsorption reactions, and that the discrete site non-electrostatic model can be used to account for proton and metal adsorption reactions. The proton-active binding sites on bacterial cell envelopes can be modeled as mono-protic acids using the following reaction (e.g., Plette et al., 1996; Fein et al., 1997):

$$R{-}A_n{-}H^0 \leftrightarrow R{-}A_n^- + H^+ \quad (1)$$

where R represents the macromolecule within the bacterial cell envelope to which each site type, A_n, is attached. These site types are operationally defined as proton-active binding sites that have similar acidity constants, and are not necessarily identical chemically within a site 'type'. The mass action equation for Reaction (1) can be expressed as:

$$K_{a-n} = \frac{\left[R{-}A_n^-\right] a_{H^+}}{\left[R{-}A_n{-}H^0\right]} \quad (2)$$

where $[R - A_n^-]$ and $[R - A_n - H^0]$ represent the concentrations of the deprotonated and protonated form of site type A_n, respectively, a_{H^+} represents the activity of H^+ in solution, and $K_{a\ -\ n}$ is the acidity constant for site type A_n. Because there have been no x-ray absorption spectroscopy studies to constrain the Mn:site binding mechanism on bacteria, we used a 1:1 Mn:site stoichiometry to account for the observed Mn(II) adsorption. This ratio is a reasonable assumption as EXAFS studies of uranium and cadmium adsorption onto bacterial cell envelope functional groups are best represented as 1:1 surface complexes (e.g., Kelly et al., 2002; Boyanov et al., 2003). The Mn(II) adsorption reaction is expressed as follows:

$$R{-}A_n^- + Mn^{2+} \leftrightarrow R{-}A_n{-}Mn^+ \quad (3)$$

where $R{-}A_n{-}Mn^+$ represents the Mn-bacterial surface complex. The corresponding mass action equation for Reaction (3) can be expressed as:

$$K_{Mn-A_n} = \frac{\left[R{-}A_n{-}Mn^+\right]}{\left[R{-}A_n^-\right] a_{Mn^{2+}}} \quad (4)$$

We use the observed extents of Mn(II) adsorption as a function of pH for a fixed Mn:biomass ratio to determine how many binding sites are involved in Mn(II) adsorption and to constrain the values of K_{Mn-A_n}. The calculations were performed using FITEQL 2.0 (Westall, 1982) with inclusion of relevant aqueous metal hydrolysis reactions, bacterial envelope reactive site concentrations and corresponding acidity constants [see Table S2 (Supplemental Material) for a list of all included reactions, equilibrium constants, and sources]. Mn^{+2} was the dominant aqueous Mn(II) species across the pH range in this study according to our modeling calculations. The thermodynamic stability constants were calculated by populating FITEQL 2.0 with the following parameters: experimental pH values, adsorbed Mn concentrations onto the bacteria of interest, and proton binding constants and site concentrations for the specific bacterial species. The proton-active functional groups within *B. subtilis* cell envelopes can be described with 4 proton-active sites with the following $pK_{a\ -\ n}$ values: 3.3 ± 0.2, 4.8 ± 0.1, 6.8 ± 0.3, and 9.1 ± 0.2 (referred to as Sites 1–4, respectively), with site concentrations of 81 ± 16, 112 ± 36, 44 ± 13 and 74 ± 21 μmol/g wet weight, respectively (Fein et al., 2005). The corresponding *P. putida* $pK_{a\ -\ n}$ values are: 3.4 ± 0.2, 4.9 ± 0.2, 6.6 ± 0.2, and 9.3 ± 0.2 with site concentration values of 103 ± 12, 77 ± 36, 112 ± 20 and 59 ± 6 μmol/g wet weight, respectively (Kenney and Fein, 2011). Given the pH range of our adsorption data, we only considered Sites 1, 2 and 3 as potential binding sites responsible for the observed Mn(II) adsorption in this study, and we tested all possible models involving Mn^{+2} binding onto one of these sites, two of these sites, and all three of these sites.

A variance parameter, V(Y), generated by FITEQL 2.0 was used to determine which model best fits the experimental data, with V(Y) values of 1 indicating a perfect fit of the model to the data (Westall, 1982). For the data collected with a Mn:biomass ratio of 3.6 μmol Mn/g wet cells, a model involving Mn^{+2} adsorption onto all three sites provided the best fit for both the *B. subtilis* and the *P. putida* data (Fig. 3). The uncertainties associated with the calculated stability constants were evaluated by determining the highest and lowest Log K_{Mn-A_n} values that encompassed approximately 95% of a given data set for a specific pH range. The uncertainties that we report denote 2σ values associated with the average Log K_{Mn-A_n} values for each site. For *B. subtilis*, the calculated thermodynamic stability constants (as Log K_{Mn-A_n}) for Sites 1, 2 and 3 are 2.8 ± 0.1, 2.9 ± 0.2, and 3.2 ± 0.1, respectively, and for *P. putida* the corresponding calculated values are 2.8 ± 0.2, 3.6 ± 0.3, and 4.0 ± 0.2, respectively. The surface speciation distribution of Mn(II) on each bacterial species is depicted in Fig. 3.

The enhanced adsorption that we observed for *P. putida* relative to *B. subtilis*, coupled with the larger Mn(II)-Site 2 and -Site 3 stability constants that reflect that enhancement, may indicate that cell envelope functional groups in *P. putida* evolved to optimize Mn(II) adsorption

Please cite this article as: Vázquez-Ortega, A., Fein, J.B., Thermodynamic modeling of Mn(II) adsorption onto manganese oxidizing bacteria, Chem. Geol. (2016), http://dx.doi.org/10.1016/j.chemgeo.2016.12.040

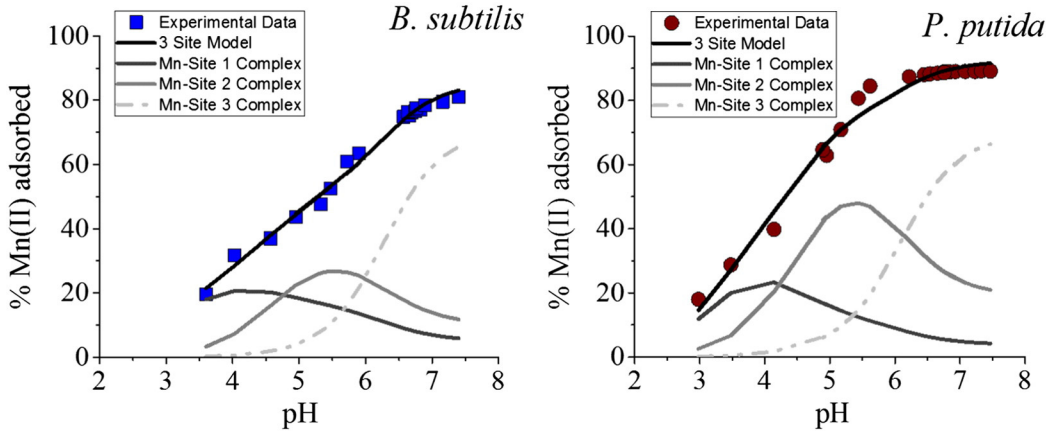

Fig. 3. Surface complexation modeling and speciation distribution results for *B. subtilis* (left) and *P. putida* (right). The *B. subtilis* and *P. putida* adsorption datasets both require Mn(II) binding onto 3 sites to account for the adsorption behavior as a function of pH, and the best-fitting model in each case is depicted as a solid black curve. This experiments were conducted with a metal:biomass ratio of 3.6 μmol Mn/g wet cells.

because of the beneficial effects of Mn to the organism. It may be advantageous for Mn-oxidizing bacteria to optimize for Mn(II) adsorption in order to promote Mn(II) oxidation. Although the exact physiological function of Mn(II) oxidation is not fully understood, the creation of Mn(IV) oxides by bacteria may contribute to energy generation for the bacteria, and the Mn(IV) oxides can act as electron acceptors under some conditions for the bacteria (Banh et al., 2013). Furthermore, Mn(IV) oxides can be beneficial to the bacteria by serving as an oxidizing agent for organic carbon compounds, or by creating a protective shield against external reactive oxygen species. Lastly, Mn(II) oxidation and production of Mn(IV) oxides by bacteria may serve to reduce the toxicity of heavy metals to the organism because these elements adsorb strongly onto Mn(IV) oxides (Nelson et al., 1999).

If the adsorption mechanism is well-characterized by Reaction 3, then the stability constants that we calculated using a specific Mn:biomass ratio should not depend on the experimental Mn:biomass ratio. In order to test this, we used the data for *P. putida* systems from each Mn:biomass ratio that we studied to calculate a new set of stability constants, and we determined whether there were significant and systematic changes to those calculated values as a function of Mn loading onto the biomass, both with and without EPS present (Figs. 4 and 5). The best-fitting models and species distribution that explained the Mn adsorption behavior onto *P. putida* with EPS as a function of both pH and Mn:biomass ratios all involved Mn^{2+} binding onto Sites 2 and 3 (Fig. 4). The calculated stability constants for Mn^{2+} binding onto Site 3 do not change significantly over the range of Mn:biomass ratios studied (Table 1, Fig. 6). Conversely, Mn-Site 2 stability constants, which are relatively constant between 5 and 40 μmol Mn/g wet cells, become smaller below 5 μmol Mn/g wet cells. Yu and Fein (2015) reported a significant increase in the value of calculated Cd-Site 3 stability constants under low metal loading conditions for *Shewanella oneidensis*, and attributed this effect to the presence of two adsorption mechanisms: one described by a high stability constant value that dominates under low metal loading conditions and involves the formation of Cd-sulfhydryl complexes within the cell envelope, and another described by a lower stability constant value that dominates under high metal loading conditions and involves Cd binding onto 'non-sulfhydryl' sites. The values of the calculated stability constants in this study do not increase

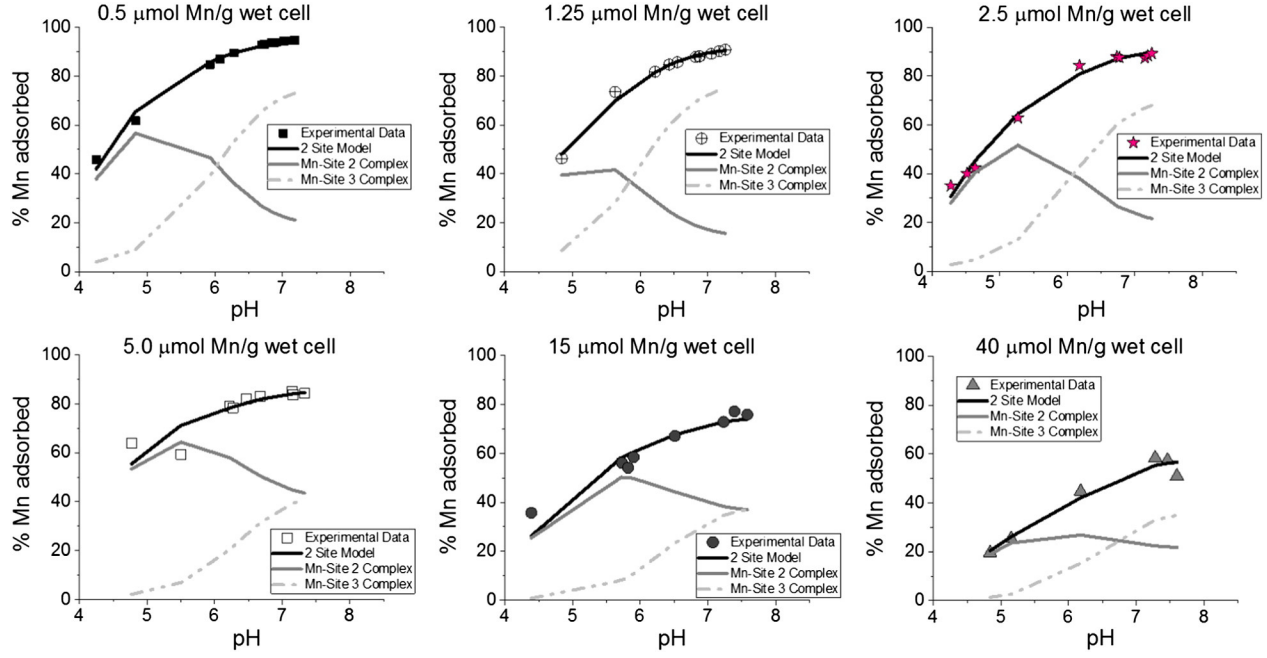

Fig. 4. Surface complexation modeling and speciation distribution results for *P. putida* containing EPS. The *P. putida* adsorption dataset requires Mn(II) binding onto 2 sites to account for the adsorption behavior as a function of both pH and metal loading.

Please cite this article as: Vázquez-Ortega, A., Fein, J.B., Thermodynamic modeling of Mn(II) adsorption onto manganese oxidizing bacteria, Chem. Geol. (2016), http://dx.doi.org/10.1016/j.chemgeo.2016.12.040

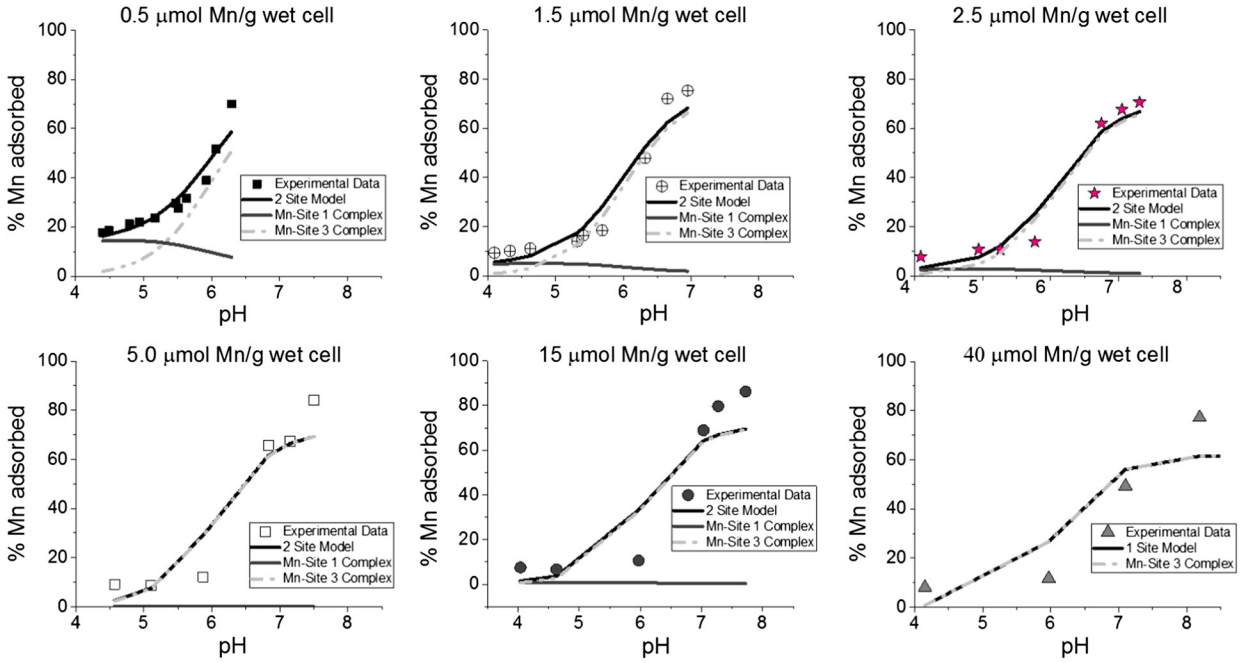

Fig. 5. Surface complexation modeling and speciation distribution results for *P. putida* with EPS removed. The dataset requires Mn(II) binding onto 2 sites to account for the adsorption behavior as a function of pH and metal loading, with the exception of the 40 µmol/g dataset. The best fit for the metal:biomass ratio of 40 µmol Mn/g wet cells was obtained with Mn binding onto Site 3 only.

significantly with decreasing metal loading, providing circumstantial but strong evidence that sulfhydryl sites do not play a role in Mn(II) binding onto *P. putida* under the range of Mn:biomass ratios examined in this study and similar to the Cd:biomass ratios studied by Yu and Fein (2015). Although *P. putida* contains similar concentrations of sulfhydryl sites to a range of other bacteria that have been studied, including *Shewanella oneidensis* (Yu and Fein, 2015), our results suggest that bacterial sulfhydryl sites have a significantly lower affinity for Mn(II) than they do for Cd(II).

Mn^{2+} binding onto two sites was required in order to model the data from the experiments with *P. putida* with the EPS molecules removed (Fig. 5). However, unlike for the EPS-bearing system, the best-fitting models for each Mn:biomass ratio studied for the EPS-free data involved Sites 1 and 3 instead of Sites 2 and 3. The calculated Mn-Site 1 stability constant values are constant as a function of metal loading over the entire range of metal loadings studied (Fig. 6). In contrast, the calculated Mn-Site 3 stability constant values decrease consistently with decreasing metal loading, with the largest decreases occurring between 0.5 and 5.0 µmol Mn/g wet biomass. The consistent decrease in the Log $K_{Mn\text{-}Site\ 3}$ values with decreasing metal loading suggests that under low Mn loading conditions Mn is bound via a reaction that has a lower binding affinity than the one that occurs under higher Mn loadings conditions. One possibility that would explain the observed trend would be a change from inner sphere binding above approximately 10 µmol Mn/g wet cells to outer sphere binding under lower Mn loading conditions. Mn(II) binding onto bacterial sulfhydryl sites would not explain the observed trends in Log $K_{Mn\text{-}Site\ 3}$ values because under the low metal loading conditions where the low-abundance sulfhydryl sites might dominate, we would expect an elevated calculated Log $K_{Mn\text{-}Site\ 3}$ value rather than the decrease that we observed. Spectroscopic studies of the molecular-scale mechanisms involved in Mn(II) binding onto bacterial cell envelopes and EPS molecules are needed in order to confirm the exact nature of the different binding sites that our data suggest. Several studies have reported no effect on Cd adsorption after EPS removal using a similar EPS removal approach to the one presented in this study (Ueshima et al., 2008; Kenney and Fein, 2011), while other studies note a decrease in the extent of metal adsorption when EPS is removed (Wei et al., 2011; Fang et al., 2014). The different observed effects of EPS removal in these studies are likely related to the specific nature of the metals involved in the adsorption studies as well as their binding affinities to the reactive sites on the EPS and within the cell envelope. Also, the experiments reported by Ueshima et al. (2008) and Kenney and Fein (2011) were conducted under high metal loading conditions only, and these conditions might mask the effects of EPS removal on metal adsorption.

Table 1
Best-fitting calculated stability constants for Mn(II)-*P. putida* complexes as a function of metal loading.

	Log K_{Mn-A_n}			
	P. putida with EPS		*P. putida* without EPS	
Metal loading (µmol Mn/g wet cells)	Site 2	Site 3	Site 1	Site 3
0.5	3.5	4.0	2.1	3.4
1.25	3.6	4.2	2.0	3.7
2.5	4.0	4.4	2.0	3.9
5	4.3	4.2	1.0	4.1
15	4.3	4.2	2.0	4.4
40	4.3	4.4	–[a]	4.7
Average	**4.0**	**4.2**	**1.8**	**4.0**
Standard deviation	**0.4**	**0.2**	**0.5**	**0.5**

[a] The best fit for the metal:biomass ratio of 40 µmol Mn/g wet cells was obtained with Mn binding onto Site 3 only.

4. Conclusion

Our experimental and modeling results indicate that a Mn(II)-oxidizing bacterial species (*P. putida*) exhibits enhanced Mn(II) adsorption behavior relative to a non-Mn(II)-oxidizing species (*B. subtilis*), perhaps as a result of evolutionary changes to *P. putida* that optimize for the uptake of beneficial Mn(II). Some experiments were conducted with biomass from which EPS molecules were removed, and these results indicated that the EPS produced by *P. putida* exerts a significant effect on the Mn(II) adsorption behavior, with the extent of adsorption decreasing significantly when EPS was removed. We modeled the data from the experiments involving *P. putida* with and without EPS

Please cite this article as: Vázquez-Ortega, A., Fein, J.B., Thermodynamic modeling of Mn(II) adsorption onto manganese oxidizing bacteria, Chem. Geol. (2016), http://dx.doi.org/10.1016/j.chemgeo.2016.12.040

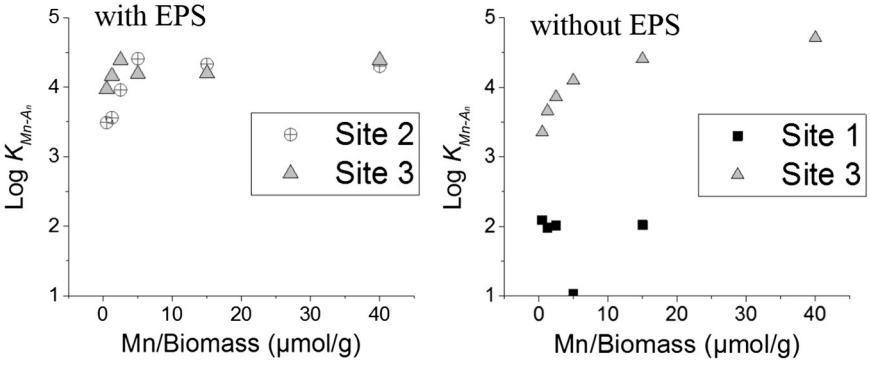

Fig. 6. Calculated stability constants (Log K_{Mn-A_n}) for Mn(II)-bacterial cell envelope site complexes as a function of metal loading conditions. The thermodynamic stability constants were calculated for *P. putida* species containing EPS (left graph) and with EPS removed (right graph). At the highest Mn:biomass ratio in the EPS-free system, Mn binding onto Site 1 was not needed to describe the experimental data.

molecules and as a function of pH and Mn:biomass ratio using two distinct Mn-adsorbing sites but with only one adsorption reaction for each site. Although in each case, the values of one of the two calculated stability constants do not change significantly as a function of Mn:biomass ratio, the calculated values of the other stability constant decreases with decreasing Mn loading onto the bacteria. This decrease provides strong circumstantial evidence for a change in binding mechanism under different Mn loading conditions, but is not likely to represent the metal-sulfhydryl binding that can dominate low metal-loading conditions for other metals and bacteria (Yu and Fein, 2016). In our study, the results from the experiments involving low Mn loading conditions suggest a relatively weaker bond forming than occurs under higher Mn loading conditions, and hence the decrease in calculated stability constant values with decreasing Mn loading. The opposite would be expected if Mn-sulfhydryl binding dominated under low Mn loading conditions. A possibility that could explain these modeling results would be the formation of an outer sphere Mn-bacterial complex under low Mn loading conditions, transitioning to inner sphere complexation under higher Mn loadings, however spectroscopic evidence is required in order to test this hypothesis. The experimental and modeling results from this study suggest that exceptions to the universal adsorption behavior proposed by Yee and Fein (2001) may exist, and that some bacteria may exhibit enhanced binding of metabolically beneficial cations.

Acknowledgements

We would like to thank guest editor Yu Yang and the journal reviewers for careful and thorough reviews of the manuscript which significantly improved the presentation of the research. This project was sponsored by the Center for Environmental Science and Technology at University of Notre Dame and National Science Foundation grant EAR-1424950.

Appendix A. Supplementary data

Supplementary data to this article can be found online at http://dx.doi.org/10.1016/j.chemgeo.2016.12.040.

References

Armstrong, P.B., Lyons, W.B., Gaudette, H.E., 1979. Application of formaldoxime colorimetric method for the determination of manganese in the pore water of anoxic estuarine sediments. Estuaries 2 (3), 198–201.

Baker, M.G., Lalonde, S.V., Konhauser, K.O., Foght, J.M., 2010. Role of extracellular polymeric substances in the surface chemical reactivity of *Hymenobacter aerophilus*, a psychrotolerant bacterium. Appl. Environ. Microbiol. 76 (1), 102–109.

Banh, A., Chavez, V., Doi, J., Nguyen, A., Hernandez, S., Ha, V., Jimenez, P., Espinoza, F., Johnson, H.A., 2013. Manganese (Mn) oxidation increases intracellular Mn in *Pseudomonas putida* GB-1. PLoS One 8 (10), 1–8.

Borrok, D.M., Fein, J.B., 2005. The impact of ionic strength on the adsorption of protons, Pb, Cd, and Sr onto the surfaces of gram negative bacteria: testing non-electro static, diffuse, and triple-layer models. J. Colloid Interface Sci. 286 (1), 110–126.

Boyanov, M.I., Kelly, S.D., Kemner, K.M., Bunker, B.A., Fein, J.B., Fowle, D.A., 2003. Adsorption of cadmium to *Bacillus subtilis* bacterial cell walls: a pH-dependent X-ray absorption fine structure spectroscopy study. Geochim. Cosmochim. Acta 67 (18), 3299–3311.

Celik, G.Y., Aslim, B., Beyatli, Y., 2008. Characterization and production of the exopolysaccharide (EPS) from *Pseudomonas aeruginosa* G1 and *Pseudomonas putida* G12 strains. Carbohydr. Polym. 73 (1), 178–182.

Czajka, D.R., Lion, L.W., Shuler, M.L., Ghiorse, W.C., 1997. Evaluation of the utility of bacterial extracellular polymers for treatment of metal-contaminated soils: polymer persistence, mobility, and the influence of lead. Water Res. 31 (11), 2827–2839.

Fang, L.C., Wei, X., Cai, P., Huang, Q.Y., Chen, H., Liang, W., Rong, X.M., 2011. Role of extracellular polymeric substances in Cu(II) adsorption on *Bacillus subtilis* and *Pseudomonas putida*. Bioresour. Technol. 102 (2), 1137–1141.

Fang, L.C., Yang, S.S., Huang, Q.Y., Xue, A.F., Cai, P., 2014. Biosorption mechanisms of Cu(II) by extracellular polymeric substances from *Bacillus subtilis*. Chem. Geol. 386, 143–151.

Fein, J.B., 2016. Advanced biotic ligand models: using surface complexation modeling to quantify metal bioavailability to bacteria in geologic systems. Chem. Geol. (in press).

Fein, J.B., Daughney, C.J., Yee, N., Davis, T.A., 1997. A chemical equilibrium model for metal adsorption onto bacterial surfaces. Geochim. Cosmochim. Acta 61 (16), 3319–3328.

Fein, J.B., Boily, J.F., Yee, N., Gorman-Lewis, D., Turner, B.F., 2005. Potentiometric titrations of *Bacillus subtilis* cells to low pH and a comparison of modeling approaches. Geochim. Cosmochim. Acta 69 (5), 1123–1132.

Flynn, S.L., Szymanowski, J.E.S., Fein, J.B., 2014. Modeling bacterial metal toxicity using a surface complexation approach. Chem. Geol. 374, 110–116.

Geszvain, K., Butterfield, C., Davis, R.E., Madison, A.S., Lee, S.W., Parker, D.L., Soldatova, A., Spiro, T.G., Luther, G.W., Tebo, B.M., 2012. The molecular biogeochemistry of manganese(II) oxidation. Biochem. Soc. Trans. 40, 1244–1248.

Gonzalez, A.G., Shirokova, L.S., Pokrovsky, O.S., Emnova, E.E., Martinez, R.E., Santana-Casiano, J.M., Gonzalez-Davila, M., Pokrovski, G.S., 2010. Adsorption of copper on *Pseudomonas aureofaciens*: protective role of surface exopolysaccharides. J. Colloid Interface Sci. 350 (1), 305–314.

Gonzalez, A.G., Pokrovsky, O.S., Jimenez-Villacorta, F., Shirokova, L.S., Santana-Casiano, J.M., Gonzalez-Davila, M., Emnova, E.E., 2014. Iron adsorption onto soil and aquatic bacteria: XAS structural study. Chem. Geol. 372, 32–45.

Guibaud, G., Comte, S., Bordas, F., Dupuy, S., Baudu, M., 2005. Comparison of the complexation potential of extracellular polymeric substances (EPS), extracted from activated sludges and produced by pure bacteria strains, for cadmium, lead and nickel. Chemosphere 59 (5), 629–638.

Guiné, V., Spadini, L., Sarret, G., Muris, M., Delolme, C., Gaudet, J.P., Martins, J.M.F., 2006. Zinc sorption to three gram-negative bacteria: combined titration, modeling, and EXAFS study. Environ. Sci. Technol. 40 (6), 1806–1813.

Gutierrez, T., Biller, D.V., Shimmield, T., Green, D.H., 2012. Metal binding properties of the EPS produced by *Halomonas* sp TG39 and its potential in enhancing trace element bioavailability to eukaryotic phytoplankton. Biometals 25 (6), 1185–1194.

Huang, J.H., Elzinga, E.J., Brechbuchl, Y., Voegelin, A., Kretzschmar, R., 2011. Impacts of *Shewanella putrefaciens* strain CN-32 cells and extracellular polymeric substances on the sorption of As(V) and As(III) on Fe(III)-(Hydr)oxides. Environ. Sci. Technol. 45 (7), 2804–2810.

Huang, F., Guo, C.L., Lu, G.N., Yi, X.Y., Zhu, L.D., Dang, Z., 2014. Bioaccumulation characterization of cadmium by growing *Bacillus cereus* RC-1 and its mechanism. Chemosphere 109, 134–142.

Jensen-Spaulding, A., Cabral, K., Shuler, M.L., Lion, L.W., 2004. Predicting the rate and extent of cadmium and copper desorption from soils in the presence of bacterial extracellular polymer. Water Res. 38 (9), 2231–2240.

Kantar, C., Demiray, H., Dogan, N.M., 2011. Role of microbial exopolymeric substances (EPS) on chromium sorption and transport in heterogeneous subsurface soils: II. Binding of Cr(III) in EPS/soil system. Chemosphere 82 (10), 1496–1505.

Kelly, S.D., Bunker, B.A., Fein, J.B., Fowle, D.A., Yee, N., Kemner, K.M., 2001. XAFS determination of the bacterial cell wall functional groups responsible for complexation of Cd and U as a function of pH. J. Synchrotron Radiat. 8, 946–948.

Kelly, S.D., Kemner, K.M., Fein, J.B., Fowle, D.A., Boyanov, M.I., Bunker, B.A., Yee, N., 2002. X-ray absorption fine structure determination of pH-dependent U-bacterial cell wall interactions. Geochim. Cosmochim. Acta 66 (22), 3855–3871.

Kenney, J.P.L., Fein, J.B., 2011. Importance of extracellular polysaccharides on proton and Cd binding to bacterial biomass: a comparative study. Chem. Geol. 286 (3–4), 109–117.

Liu, H., Fang, H.H.P., 2002. Characterization of electrostatic binding sites of extracellular polymers by linear programming analysis of titration data. Biotechnol. Bioeng. 80 (7), 806–811.

Nelson, Y.M., Lion, L.W., Ghiorse, W.C., Shuler, M.L., 1999. Production of biogenic Mn oxides by *Leprothrix discophora* SS-1 in a chemically defined growth medium and evaluation of their Pb adsorption characteristics. Appl. Environ. Microbiol. 65 (1), 175–180.

Ngwenya, B.T., Sutherland, I.W., Kennedy, L., 2003. Comparison of the acid-base behaviour and metal adsorption characteristics of a gram-negative bacterium with other strains. Appl. Geochem. 18 (4), 527–538.

Plette, A.C.C., Benedetti, M.F., Van Riemsdik, W.H., 1996. Competitive binding of protons, calcium, cadmium, and zinc to isolated cell walls of a gram-positive soil bacterium. Environ. Sci. Technol. 30 (6), 1902–1910.

Raungsomboon, S., Chidthaisong, A., Bunnag, B., Inthorn, D., Harvey, N.W., 2006. Production, composition and Pb^{2+} adsorption characteristics of capsular polysaccharides extracted from a cyanobacterium *Gloeocapsa gelatinosa*. Water Res. 40 (20), 3759–3766.

Sheng, G.P., Yu, H.Q., Yu, Z., 2005. Extraction of extracellular polymeric substances from the photosynthetic bacterium *Rhodopseudomonas acidophila*. Appl. Microbiol. Biotechnol. 67 (1), 125–130.

Sheng, L., Szymanowski, J., Fein, J.B., 2011. The effects of uranium speciation on the rate of U(VI) reduction by *Shewanella oneidensis* MR-1. Geochim. Cosmochim. Acta 75 (12), 3558–3567.

Tebo, B.M., Geszvain, K., Lee, S., 2010. The molecular geomicrobiology of bacterial manganese(II) oxidation. In: Barton, L.L., Mandl, M., Loy, A. (Eds.), Geomicrobiology: Molecular and Environmental Perspective. Springer, Berlin, pp. 285–308.

Tourney, J., Ngwenya, B.T., Mosselmans, J.W.F., Magennis, M., 2009. Physical and chemical effects of extracellular polymers (EPS) on Zn adsorption to *Bacillus licheniformis* S-86. J. Colloid Interface Sci. 337 (2), 381–389.

Ueshima, M., Ginn, B.R., Haack, E.A., Szymanowski, J.E.S., Fein, F.B., 2008. Cd adsorption onto *Pseudomonas putida* in the presence and absence of extracellular polymeric substances. Geochim. Cosmochim. Acta 72 (24), 5885–5895.

Wei, X., Fang, L.C., Cai, P., Huang, Q.Y., Chen, H., Liang, W., Rong, X.M., 2011. Influence of extracellular polymeric substances (EPS) on Cd adsorption by bacteria. Environ. Pollut. 159 (5), 1369–1374.

Westall, J.C., 1982. FITEQL, A Computer Program for Determination of Chemical Equilibrium Constants from Experimental Data. Version 2.0. Report 82-02. Department of Chemistry, Oregon State University.

Wu, S.C., Luo, Y.M., Cheung, K.C., Wong, M.H., 2006. Influence of bacteria on Pb and Zn speciation, mobility and bioavailability in soil: A laboratory study. Environ. Pollut. 144 (3), 765–773.

Yang, S.Y., Ngwenya, B.T., Butler, I.B., Kurlanda, H., Elphick, S.C., 2013. Coupled interactions between metals and bacterial biofilms in porous media: IMPLICATIONS for biofilm stability, fluid flow and metal transport. Chem. Geol. 337, 20–29.

Yee, N., Fein, J., 2001. Cd adsorption onto bacterial surfaces: a universal adsorption edge? Geochim. Cosmochim. Acta 65 (13), 2037–2042.

Yee, N., Fein, J.B., 2002. Does metal adsorption onto bacterial surfaces inhibit or enhance aqueous metal transport? Column and batch reactor experiments on Cd-*Bacillus subtilis*-quartz systems. Chem. Geol. 185 (3–4), 303–319.

Yu, Q., Fein, J.B., 2015. The effect of metal loading on Cd adsorption onto *Shewanella oneidensis* bacterial cell envelopes: the role of sulfhydryl sites. Geochim. Cosmochim. Acta 167, 1–10.

Yu, Q., Fein, J.B., 2016. Sulfhydryl binding sites within bacterial extracellular polymeric substances. Environ. Sci. Technol. 50 (11), 5498–5505.

Yu, Q., Szymanowski, J., Myneni, S.C.B., Fein, J.B., 2014. Characterization of sulfhydryl sites within bacterial cell envelopes using selective site-blocking and potentiometric titrations. Chem. Geol. 373, 50–58.

Please cite this article as: Vázquez-Ortega, A., Fein, J.B., Thermodynamic modeling of Mn(II) adsorption onto manganese oxidizing bacteria, Chem. Geol. (2016), http://dx.doi.org/10.1016/j.chemgeo.2016.12.040